An upright life, the postural stability of birds: a tensegrity system

Anick Abourachid, Christine Chevallereau, Idriss Pelletan, Philippe Wenger

An upright life, the postural stability of birds : a tensegrity system

Anick Abourachid [1]., Christine Chevallereau [2] , Idriss Pelletan[1], Philippe Wenger [2]

https://royalsocietypublishing.org/doi/10.1098/rsif.2023.0433 .

1 Muséum National d'Histoire Naturelle CNRS, Mecadev, 57 rue Cuvier 75231 Paris cedex 05.

2 Nantes Université, Centrale Nantes, CNRS, LS2N, 44000 Nantes, France

AA :ORCID iD : 0000-0002-7238-2795 ; CC: ORCID iD **:** 0000-0002-1929-5211; PW ORCID iD : 0000-0002-6608-4484

Abstract

Birds are so stable that they can rest and even sleep standing up. We propose that stable static balance is achieved by tensegrity. The rigid bones can be held together by tension in the tendons, allowing the system to stabilise under the action of gravity. We used the proportions of the bird's osteomuscular system to create a mathematical model. First, the extensor muscles and tendons of the leg are replaced by a single cable that follows the leg and is guided by joint pulleys. Analysis of the model shows that it can achieve balance. However, it does not match the biomechanical characteristics of the bird's body and is not stable. We then replaced the single cable with four cables, roughly corresponding to the extensor groups, and added a ligament loop at the knee. The model is then able to reach a stable equilibrium and the biomechanical characteristics are satisfied. Some of the anatomical features used in our model correspond to innovations unique to the avian lineage. We propose that tensegrity, which allows light and stable mechanical systems, is fundamental to the evolution of the avian body plan. It can also be used as an alternative model for bipedal robots.

Key words : Bird - static equilibrium- evolution - robotic

Main text

The 10,000 bird species share strict bipedalism with one mammal, *Homo sapiens*. The fundamental difference is that avian bipedalism is flexed, whereas human bipedalism is upright. The flexed bipedalism of birds gives them such stability that they can perch on substrates such as thin branches or electrical wires. The upright human postural stability is largely based on a compressive skeletal organisation (Figure 1), with lines of force propagating through the bones (Carter et al 1987). The support of the structure requires a very precise adjustment of the skeletal elements, thanks to the curvatures of the spine and the peculiar shape of the pelvis, which distributes the mechanical constraints towards the two legs that form pillars (Tardieux 2013). The musculature is required to adjust the orientation of the bony segments (Do Rosário 2014). People tend to rest sitting or lying down. The body structure of birds is different (Fig. 1). Under a thick plumage, the legs support a rigid trunk with a short bony tail, the wings and the head at the end of a long neck. The legs are more or less long, but the structure is always the same, with three long bones plus toes. The musculature of the back is reduced due to the bony stiffening of the spine (Raikow 1985). The powerful wing muscles are carried ventrally on the sternum. The sternum is very large, usually with a keel to increase the surface area for the pectoral muscles that move the wing for flight. The musculature of the thigh is very large, as is that of the calf. There are very few fleshy muscles below the ankle, but long tendons that connect to the toes (Raikow 1985). The trunk is oblique, the hip and knee are always flexed, and the distribution of muscle mass places the centre of mass of the body well forward of the hip (Allen 2013), between the two knees when the birds are standing (Abourachid 1993). This position of the centre of mass towards the

centre of the trunk is critical for flight (Harvey & al 2022). The avian leg is a very versatile system. In addition to locomotion (walking, running, swimming, taking off, landing) in a variety of environments, they can be used for grasping food or for predation (Abourachid & Hofling 2012). Phylogeny and the diversity of living environments and behaviours imply morphological adaptations of the osteo-muscular system to meet functional constraints. However, postural stability is a fundamental trait shared by all birds. The osteo-muscular system is sufficiently stable to allow birds to sleep upright (Galton et al 2012), their preferred resting position. They are seen standing still on a wire or soft branch, even in the wind. The system is sufficiently balanced to allow them to sleep standing on one leg (Chang and Ting 2017). We therefore hypothesised that stability could be achieved at minimal energy cost, i.e. with almost no muscular effort through passive tension. Our approach aims to overcome specific differences to reveal possible intrinsic properties of the organisational plan shared by all birds. We are looking for the characteristics of the osteomuscular system that are required to keep a standing bird stable at rest with minimal effort.

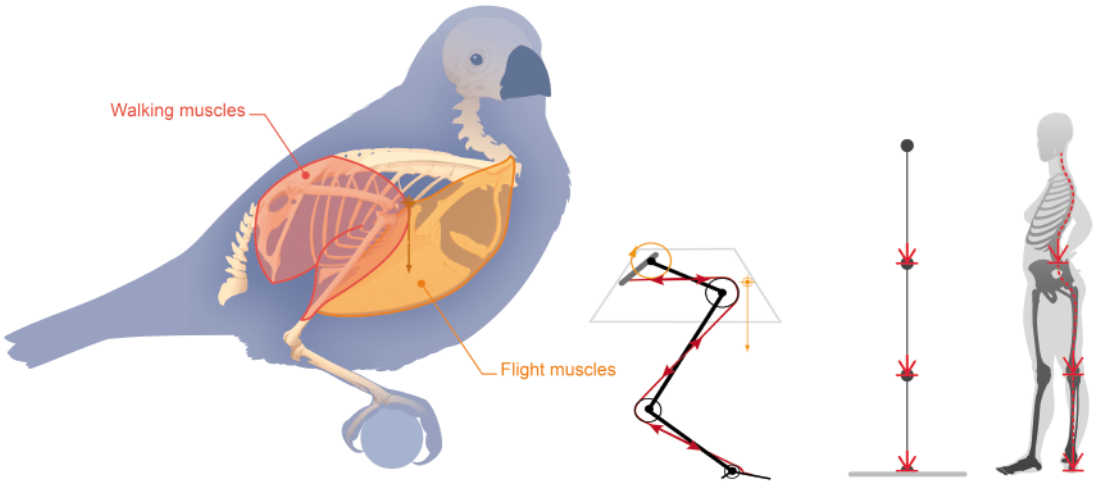

Figure 1: Bipeds: In birds, a thick plumage hides most of the body. The rigid trunk is supported by the long segmented legs, with the hip and knee always bent. Muscle mass is mainly distributed between the flight muscles at the front and the leg muscles at the back, with the centre of mass between the two. Human bipedalism relies on upright compressive skeletal organization, with forces propagating through the bones and precise adjustments made through vertebral curvatures and the shape of the pelvis. (Drawing by Camille Degardin).

Because the joints are highly flexed, the postural stability of birds cannot be understood as a compressive system like the human bipedal system. An alternative system is tensegrity. Tensegrity is defined as a system of rigid bodies that are held together by stresses. Tensegrity systems are lightweight and flexible. Originally used by artists, then in architecture, they are defined as a self-stressing mechanical structure composed of rigid elements in compression (rods) and elements in tension that are not rigid in compression (cables and/or springs). The prestressed state is achieved by pretensioning the cables or springs. This state provides a stable equilibrium for the tensegrity structure (Snelson 1965). They are used in architecture, for example in the construction of bridges suspended by cables. For biological systems, Ingberg and colleagues (2014) propose to define tensegrity as a structure in which a synergy between tensions and compressions creates a tensile stress that stabilises the whole structure in 3D. This definition is very broad, as the presence of cables and rigid bodies is not mandatory for a system to be defined as tensegrity. It can then be identified from micro to macroscopic scales, from molecular to organismal levels. Tensions can arise from atomic forces of attraction (molecular level) as well as from muscles or tendons at the level of the osteomuscular system. Compressive elements can be microtubules in cells or bones for the osteomuscular system (Swanson 2013). We hypothesised that a tensegrity sensus Ingber (2014) can be identified in the body of the birds. Static posture and balance would be achieved through passive tension in the osteomuscular system that provides extension of the hindlimb under the action of gravity when the bird is standing.

To address this question, we use a multidisciplinary biology-robotics approach. This collaboration allows evolutionary biology to identify structural features that are uniquely associated with stability. The geometry of robotic models is free from the historical constraints associated with the evolutionary origin of the animal group, and from the structural compromises associated with the need to associate in the same mechanical system all the vital functions of a living organism (Abourachid & Hugel 2015). In robotics, this collaboration allows the analysis of an existing stable structure to test whether it could be a candidate as an alternative to current bipedal robots based on the erect human model. The difference between the resting position of a human in compression and the resting position of a bird in tensegrity is illustrated in Figure 1.

We have used an idealised theoretical framework by considering a bilaterally symmetric biomechanical system and studying this system in the sagittal plane. Like Alexander and Dimery (1985), we assume that the forces "act in a single plane, the joints are frictionless, and their movements are considered to be rotations about a centre of rotation". In addition, we have introduced pulleys into the biomechanical system. They represent the path of the cables and allow the lengthening and shortening of the cables associated with the joint movements to be calculated. The system combines 5 rigid bodies (Fig. 2): the trunk T (which includes the head and wings), the femur F, the tibiotarsus Tbt and tarsometatarsus Tmt and the toes. The system is in contact with the ground at the base of the toe III. The segments are articulated between T and F at H (hip), between F and Tbt at K (knee), between Tbt and Tmt at A (ankle) and between Tmt and the fingers at P (metatarsophalangeal joint).

The muscle and tendon system is complex. We first propose a drastic simplification by replacing all the muscles and tendons of the leg with a single cable that follows the leg, guided by the pulleys. It attaches proximally to the posterior trunk, in the geometric centre of the origin of the iliofibular muscle, on the post-acetabular part of the pelvis, and distally under the feet on the first phalanx of the toes III. (It therefore attaches to T behind H, passes in front of K, behind A and in front of P and attaches to the toe III to compensate for gravity. The direction of the cable is redirected without friction using pulleys at joints K, A and P. The cable does not run along F, and there is a rotation at the hip to model the movements of F relative to T.

The mass of the legs is negligible compared to the mass of the trunk T. We therefore consider the centre of mass (CoM) to be integral with the trunk. The CoM is in front of H (Abourachid 1991). The action of gravity will tend to rotate T clockwise around the centre of rotation of H and put tension on the cable attached to the other side of the centre of rotation of H (Fig. 2).

Based on the anatomy of birds, we designed a mathematical model to test the hypothesis of postural equilibrium and the stability of this equilibrium. This model allows us to highlight the parameters necessary for stability and to identify them among the anatomical characteristics of birds.

Material and method

Anatomical parameters (Figure 2)

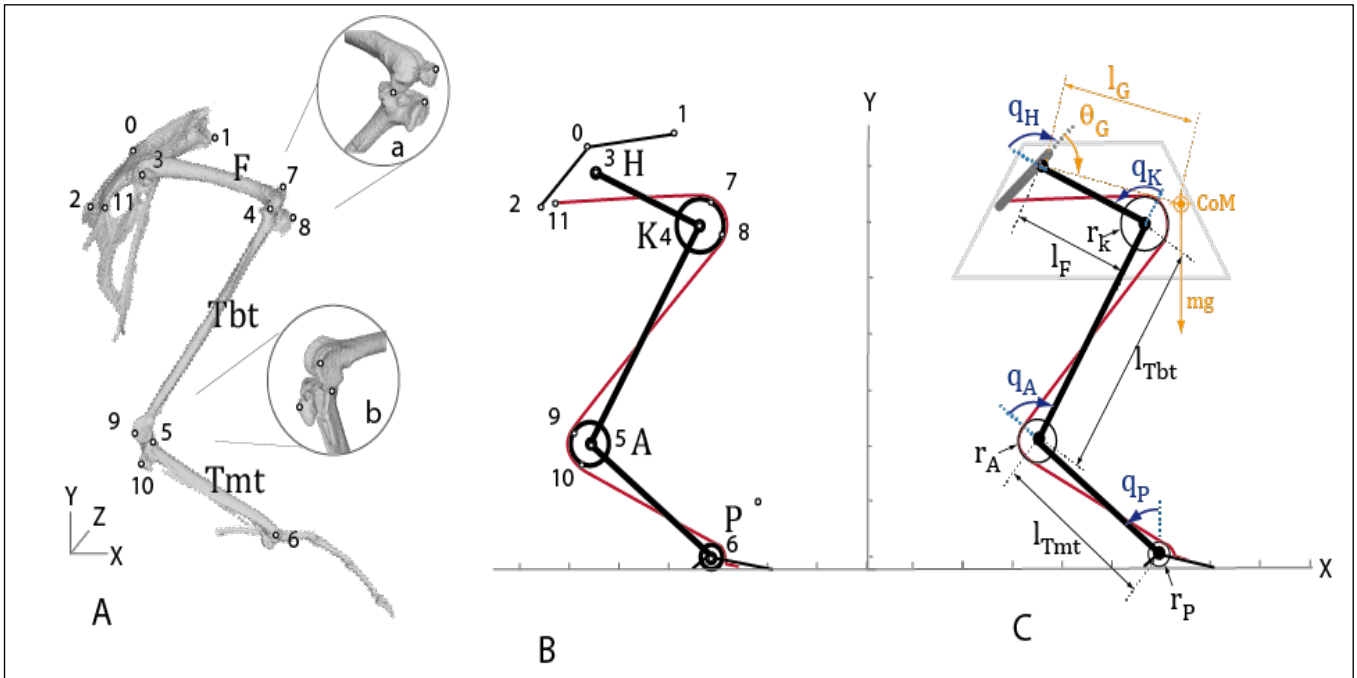

Figure 2: Construction of the one-cable model modelling

A: Lateral view of the zebrafinch's leg skeleton with anatomical landmarks used for modelling. A and b : The knee and ankle are rotated slightly to show the structures.

F: femur, Tbt: tibiotarsus, Tmt: tarsometarasus, CoM: center of mass. 0 : middle of the synsacrum, 1: Middle of the first sacral vertebrae. 2: Caudal extremity of the synsacrum. 3: Middle of the femoral head *Lig.capitis femori.,* 4: Proximal extremity of the tibiotarsus *area interarticularis.* 5: Proximal extremity of the tarsometatarsus *Eminentia intercotylari.* .6: Distal extremity of the tarsometatarsus *trochlea metatarsi* III plantar face,.7: Proximo cranial part of the patella. 8: Proximal extremity of the tarsometatarsus *Crista patellaris*. 9: Distal extremity of the tibiotarsus, caudal face *condylus lateralis.* 10: Proximal extremity tarsometarsus *Crista medialis hypotarsi*. 11: middle lateral crest ilium.

B: Modelling of the one cable system. The red cable attached on the ilium (11) caudaly to the Hip (H), passes in front of the knee (K) pulley, behind the ankle (A) pulley and in front of the foot pulley (P).

C: Dimensions used for modelling

We have used our expertise in functional anatomy to propose the generic bird model. (Fig 2A and fig 4 A)

Hip H – The trunc of the birds forms a rigid body. The dorsal vertebrae are ankylosed. The elongated pelvis is anchored to the spine by 10 to 12 sacral vertebrae (Boas, 1933) (between points 1 and 2). The head of the femur is inserted into the acetabulum of the pelvis (point 3) to form the ball and socket hip joint. The extensor muscles insert on the postacetabular part of the pelvis, (caudally to the point 3).

Knee K - The femur articulates on the posterior part of the tibial plateau (point 4). The patella (point 7), slides into the femoral groove and the patellar ligament attaches to the patellar crest of the tibiotarsus (point 8, and Fig4) (Baumel & A)Raikow 1993). We considered that the joint could be represented by a pulley centred on the posterior part of the tibial plateau at the level of the menisci (point 4), with its circumference passing through the patella, (point 7) where the knee extensors attach, and the patellar crest of the tibiotarsus (point 8), where the patellar ligament attaches (Allen & al 2017).

Ankle A - The two tibiotarsal condyles articulate on two cotyls on the anterior part of the hypotarsal plateau (point 5 and Fig4). The tendons of the toe flexor muscles pass through the ankle joint (intertarsal joint) by sliding caudally on the tibial cartilage (point 9) and into channels or grooves of the hypotarsal (Fig 4A) (Baumel 1993). We considered that the joint could be represented by a pulley centred on the hypotarsal plateau between the cotyls (point 5), with its circumference passing through the tibial cartilage (point 9) and the hypotarsal sulcus (point10).

Metatarsophalangeal joint, P - The toes of birds are very diverse in shape and orientation, but the toe III is always oriented forward (Abourachid et al. 2017, Leblanc & al. 2023). Therefore, we use in our model the articulation between the metatarsus and the first phalange of the toe III. Metatarsus III is shaped more or less anteriorly and upwardly depending on the species. The plantar surface of birds is covered by the podotheca, which covers very thick pads (fat bodies), which in turn cover the ligamento-tendinous system (Baumel & Raikow 1993). The thickness of the pad and the podotheca provides a distance between the P-joint and the substrate when the bird is in a standing position (Hofling & Abourachid 2021). We considered the centre of the pulley to be at the level of metatarsophalangeal joint III (point 6) and the circumference to be on the ground, under the podotheca.

The morphology and proportions of the zebra finch (*Taeniopygia guttata*) were used to construct the mathematical model. The resting position of the body was determined from lateral and frontal radiographs. A 3D model obtained by X-ray tomography of the whole individual, segmented bone by bone (Provini & Abourachid 2018), was used to position each bone in the resting position (Meshlab v2021 07). Landmark software (v3.0.0.6) was used to obtain the 3D Cartesian coordinates of the anatomical landmarks required to parameterise the model (Table 1, Figure 2). Three points on the sagittal plane of the bird (points 0, 1 and 2) were used as reference to calculate the coordinate of all the anatomical landmarks onto the sagittal plane. These in plane coordinates were used to parameterise the geometric model.

We estimated the location of the centre of mass using the double suspension method (Abourachid 1993). X-ray images were used to determine the position of the body segments (head, neck, trunk, wings and legs) suspended from two points. The vertical line through the suspension point passes through the centre of mass. The intersection of the straight lines of the radiographs at two positions indicates the part's centre of mass. The geometric sum of the parts' centres of mass is the body's CoM (SM 1). We graphically projected the estimated position onto the sagittal plane of the digital model.

The hypothesis of equilibrium and postural stability was tested using a mechanical approach. Matlab software was used for the various calculations. The calculations are based on a static model taking into account the effects of gravity and the stiffness of the cable (modelled as an undamped linear spring).

The equations are developed below.

			X	Y	Z
0	Sagittal plan	middle of the synsacrum	981	211	140
1	Sagittal plan	Middle of the forst sacral vertebrae	914	274	184
2	Sagittal plan	Caudal extremity of the synsacrum	1183	222	170
3	CoR hip H	*Lig.capitis femoris*	1042	192	221
4	CoR knee K	Proximal extremity of the tibiotarsus *area interarticularis*	892	259	434
5	CoR ankle A	Proximal extremity of the tarsometatarsus *Eminentia intercotylaris*	1299	411	498
6	CoR phalangeal joint P	Distal extremity of the tarsometatarsus *trochlea metatarsi* III plantar face	1188	636	668
7	Radius knee 1	Proximo cranial part of the patella	841	261	442
8	Radius knee 2	Proximal extremity of the Tarsometatarsus *Crista patellaris*	871	282	466
9	Radius ankle 1	Distal extremity of the tibiotarsus caudal face *condylus lateralis* E	1323	383	509
10	Radius ankle 2	Proximal extremity tarsometarsus *Crista medialis hypotarsi*	1334	422	520
11	Cable origin	middle lateral crest ilium,	1138	177	227

Table 1 Landmarks on the 3D model of the zebra finch skeleton.

Anatomical Nomenclature from Baumel (1986) non metric coordinates (pixels).

Results

Mathematical model with one cable

The length of the cable l connecting the attachment points on the pelvis and toe III varies according to the angles of the different joints. The variation in cable length for a joint displacement is proportional to the angle variable with a coefficient of proportionality equal to the pulley radius at P, A and K for joint angles q_P , q_A and q_K respectively. r_P , r_A , r_K are the radii of the different pulleys shown in Figure 2C. The position of the major muscles in front of or behind the knee and ankle joints is fairly clear and their placement on either side of the pulley is not controversial. The shape of the metatarsal trochlea is more complex. We introduce the term s_P, which can take a value of 1 or -1, to study the cases where the cable passes in front of or behind the centre of rotation of P. The + sign is used as soon as the cable passes in front of the pulley, increasing the joint variable in an anti-clockwise direction will result in lengthening the cable. Similarly, the - sign is used when the cable passes behind the pulley. The total length of the cable also includes a constant length noted l_0 depending on the length of the bone segments. Since the modelling in the following section essentially concerns the effect of variations in cable length, this quantity l_0 will have no impact and is therefore not further detailed here.

On the balance sheet, we have the following relationship:

$$\mathrm{l}(\boldsymbol{q}) = l_0 + s_P r_P q_P - r_A q_A + r_K q_K + l_H(q_H)$$

where $\boldsymbol{q} = [q_P \quad q_A \quad q_K \quad q_H]^T$ is the vector of joint variables.

Searching for balance

To find the equilibrium positions, we write the static equilibrium of all the bodies under the action of gravity and the elongation of the cable of stiffness K and natural spring length l_v.

In a reference frame placed under the toe at the vertical to the point P, with axis x horizontal and the axis y vertical (see figure 5). The vertical axis was measured in the space of the landmarks. An angle of 33° was found between the vertical and vector between the points 11 and 3. (see figure 2B). The position of the CoM according to the joint positions is then :

$$x_{CoM} = -l_{Tmt}\sin(q_P) - l_{Tbt}\sin(q_P + q_A) - l_F\sin(q_P + q_A + q_K) - l_G\sin(q_P + q_A + q_K + q_H + \theta_G)$$

$$y_{CoM} = r_P + l_{Tmt}\cos(q_P) + l_{Tbt}\cos(q_P + q_A) + l_F\cos(q_P + q_A + q_K) + l_G\cos(q_P + q_A + q_K + q_H + \theta_G)$$

The different lengths are shown in Figure 2C. l_G and θ_G define the position of the CoM on the trunk relative to H.

The forces acting on the system are the gravity forces and the forces in the cables (or muscles/tendons). Gravity comes from a potential energy of gravity. The energy of the force in the cable $\mathrm{F\,l}$ was modeled using Wenger & Chablat 's (2019) method.
An equilibrium position **q** minimises the potential energy $\mathrm{U}(\boldsymbol{q})$ of the system.

$$\mathrm{U}(\mathbf{q}) = \mathrm{m\,g}\, y_{CoM}(\mathbf{q}) + \mathrm{F\,l}(\mathbf{q})$$

where F is the force in the cable $F = K(l(\boldsymbol{q}) - l_v)$

This equilibrium position therefore satisfies equation : $\frac{\partial \mathrm{U}}{\partial \mathrm{q}} = 0$. This gives the following equation:

$$\begin{bmatrix} -l_{Tmt}SP - l_{Tbt}SPA - l_F SPAK - l_G SPAKG \\ -l_{Tbt}SPA - l_F SPAK - l_G SPAKG \\ -l_F SPAK - l_G SPAKG \\ -l_G SPAKG \end{bmatrix} + \begin{bmatrix} s_P r_P \\ -r_A \\ r_K \\ \frac{\partial\, l_H(q_H)}{\partial\, q_H} \end{bmatrix} \frac{\mathrm{F}}{\mathrm{mg}} = \begin{bmatrix} 0 \\ 0 \\ 0 \\ 0 \end{bmatrix} \qquad (1)$$

where

$SP = \sin(\mathrm{q_P});\ SPA = \sin(\mathrm{q_P} + \mathrm{q_A})\ ;\ SPAK = \sin(\mathrm{q_P} + \mathrm{q_A} + \mathrm{q_K});\ SPAKG = \sin(\mathrm{q_P} + \mathrm{q_A} + \mathrm{q_K} + \mathrm{q_H} + \theta_G)$

The position obtained is an equilibrium position under 2 additional conditions : the force in the cable must be positive, i.e. $l(\boldsymbol{q}) > l_v$ and $x_{CoM}(q)$ must be in the support surface of the foot, which is assumed to be horizontal.

Importance of geometry

In this equation, we see the geometric parameters of the bird's leg that affects its equilibrium position. The first vector describes the distances along the horizontal axis between the different joints and the CoM. The second vector describes the extension of the cable as the different joints move. It consists of the lever arms corresponding to the effect of the force in the cable on the different joints. When the cable is modelled using a pulley, the lever arm is constant and is defined by the radius of the pulley. Depending on the direction in which the cable passes, the moment generated will be negative or positive, which determines the signs that appear in this equation. For the hip, there are no pulleys, so the term $\frac{\partial\, l_H(q_H)}{\partial\, q_H}$ is directly the lever arm defined by the minimum distance between the hip and the cable. This term varies slightly with joint position, but is negative. To make it easier to interpret, we

will use the notation $r_H(q_H) = -\frac{\partial\, l_H(q_H)}{\partial\, q_H}$ with $r_H(q_H) > 0$. This means that we are modelling the system as if there were a pulley with radius r_H that varies according to the position of the hip.

The equations can be rewritten as:

$$\begin{bmatrix} x_{CoM} - x_P \\ x_{CoM} - x_A \\ x_{CoM} - x_K \\ x_{CoM} - x_H \end{bmatrix} = \begin{bmatrix} -s_P r_P \\ r_A \\ -r_K \\ r_H(q_H) \end{bmatrix} \frac{\mathrm{F}}{\mathrm{mg}} \qquad (2)$$

The term $\frac{\mathrm{F}}{\mathrm{mg}}$ is a dimensionless term. It expresses the ratio between the tension in the cable and the weight of the bird. Its value is around 1. This term can be varied to adjust the equilibrium position, but it can only be positive, otherwise equilibrium is not possible.

By combining the equations we can also have information about the relative equilibrium positions of the different joints:

$$\begin{bmatrix} x_A - x_P \\ x_K - x_A \\ x_H - x_K \end{bmatrix} = \begin{bmatrix} -s_P r_P - r_A \\ r_A + r_K \\ -r_K - r_H(q_H) \end{bmatrix} \frac{\mathrm{F}}{\mathrm{mg}} \qquad (3)$$

We will first interpret these equations assuming that the terms r_P , r_A , r_K , r_H are positive and correspond to the radii of the pulleys shown in Figure 2.

Equations (2) and (3) then show us that the only possible equilibrium configurations have the following properties:

1) From the first line of equation (2) it can be seen that r_P defines the vertical projection, along x, of the distance between the centre of mass and point P. The radius r_P must therefore be small; this ensures that the mechanical equilibrium condition of not tilting the bird is satisfied. Depending on the sign of s_P, the projection of the CoM will be in front of or behind P, the centre of rotation of the toe joint on the tarsometatarsus. If the cable passes in front of (or behind) the pulley, the x-projection of the CoM will be behind (or in front of) the toe joint (Fig.3)

2) From lines 2 to 4 of equation (2), it can be seen that along the horizontal x-axis the CoM is at the back of the knee K and at the front of the ankle and hip. The horizontal distance between the joints and the projection of the CoM is directly proportional to the size of the pulleys of the different joints.

3) The first line of equation (3) shows that the tibia is more inclined (or more vertical) when the cable passes in front of (or behind) the pulley r_P (see figure 3).

The equilibrium equations give us a number of constraints on the position of the joints along the x axis. The vertical arrangement is then directly related to the length of the bodies and the length of the cable.

Equilibrium can exist for a wide range of different geometries characterized by different values for s_P, r_P, r_A, r_K, l_{Tmt}, l_{Tbt}, l_F, l_G, θ_G which can be calculated using the Matlab code supplied with SM 3. The relative size of the pulleys and the trajectory of the cable at the foot influence the orientation of the segments at equilibrium and the required tension in the cable.. With our anatomical parameters it is possible to find different configurations of equilibrium if the parameters *l_G, θ_G are properly adapted as shown in figure 3. However, based on equation (2), with $r_K > 0$ i.e. the cable passing in front of the knee, the CoM along the X-axis must be at the back of the knee (see Figure 3). Since it*

is observed in the zebra finch that the CoM along the X-axis is in front of the knee, a condition needed for stabilizing the flight, (see Figure 1), the equilibrium given by the model is not coherent with the biological observation. In order to have the centre of mass located at the front of the knee, the cable would have to pass behind the knee pulley

Postural stability

The bird's equilibrium is subject to 2 types of instability. A mechanical instability: if the CoM is projected outside the toes support zone, the leg will tilt around a limit of the support zone. This instability is characterized by the geometry of the equilibrium as seen previously. The second one is instability in face of disturbances. Faced with a tiny disturbance in the configuration of the leg, will it return to its equilibrium position under the action of the elastic cable, or will it move away from it? This instability is characterized by the system's potential energy. That is what this section is all about.

The stifness $\boldsymbol{K} = \frac{\partial^2 U(\boldsymbol{q})}{\partial^2 \boldsymbol{q}}$ is positive for stable equilibrium. For our 4-joint system, the stiffness matrix is a (4 x 4) matrix with each term defined by : $K_{i,j} = \frac{\partial^2 U(\boldsymbol{q})}{\partial q_i \, \partial q_j}$.

The system studied includes only gravity and cable stiffness terms. The stiffness matrix is decomposed into 2 contributions:

$$\boldsymbol{K} = \boldsymbol{K_g} + \boldsymbol{K_c} \qquad (4)$$

where $\boldsymbol{K_g}$ contains the contribution of gravity and $\boldsymbol{K_c}$ the contribution of the cable.

The matrix $\boldsymbol{K_g}$ is written as:

$$\boldsymbol{K_g} = -mg \begin{bmatrix} y_P & y_A & y_K & y_H \\ y_A & y_A & y_k & y_H \\ y_K & y_K & y_K & y_H \\ y_H & y_H & y_H & y_H \end{bmatrix} \qquad (5)$$

Where y_i is the distance between joint i and the position of the CoM along the vertical axis. For our bird in equilibrium, the CoM is at the knee, so the distances y_P and y_A are positive, while y_K and y_H are negative. As a result, we observe instabilities due to the effect of gravity on the toe and ankle joints.

For the system studied with a single long cable, and taking $\boldsymbol{K_c}$ as the cable stiffness, the stiffness matrix has the form:

$$\boldsymbol{K_c} = \begin{bmatrix} Kr_P^2 & -Kr_P r_A & Kr_P r_K & Kr_P r_H(q_H) \\ -Kr_P r_A & Kr_A^2 & -Kr_A r_K & -Kr_A r_H(q_H) \\ Kr_P r_K & -Kr_A r_K & Kr_K^2 & Kr_K r_H(q_H) \\ Kr_P r_H(q_H) & -Kr_A r_H(q_H) & Kr_K r_H(q_H) & K\left(r_H^2(q_H) + \frac{\partial l_H^2(q_H)}{\partial^2 q_H}(l - l_v)\right) \end{bmatrix}$$

It can be shown that there is no choice of morphological parameters that allows a stable equilibrium. Without going into details, since the matrix $\boldsymbol{K} = \boldsymbol{K_g} + \boldsymbol{K_c}$ is positive, all the determinants of the minors must be positive. If we are interested in the submatrix (2 x2) associated with the toe and ankle joints, the matrix $\boldsymbol{K_g}$ associated with the negative terms and the associated matrix $\boldsymbol{K_c}$ must provide stability. In fact, the CoM is higher than the toe and ankle joints, and the system is an inverse pendulum that is not stable under the action of gravity. With a single cable passing through both joints, the cable cannot prevent an internal falling movement where q_P and q_A would go in different directions without changing the length of the cable. The mathematical development is available at supplementary material [SM 2].

The single-cable system achieves equilibrium, but this equilibrium is not resistant to perturbations.

We will therefore turn to a more complex model to see if a four-cable system, similar to the extensor muscles of the bird's joints, can achieve a stable equilibrium.

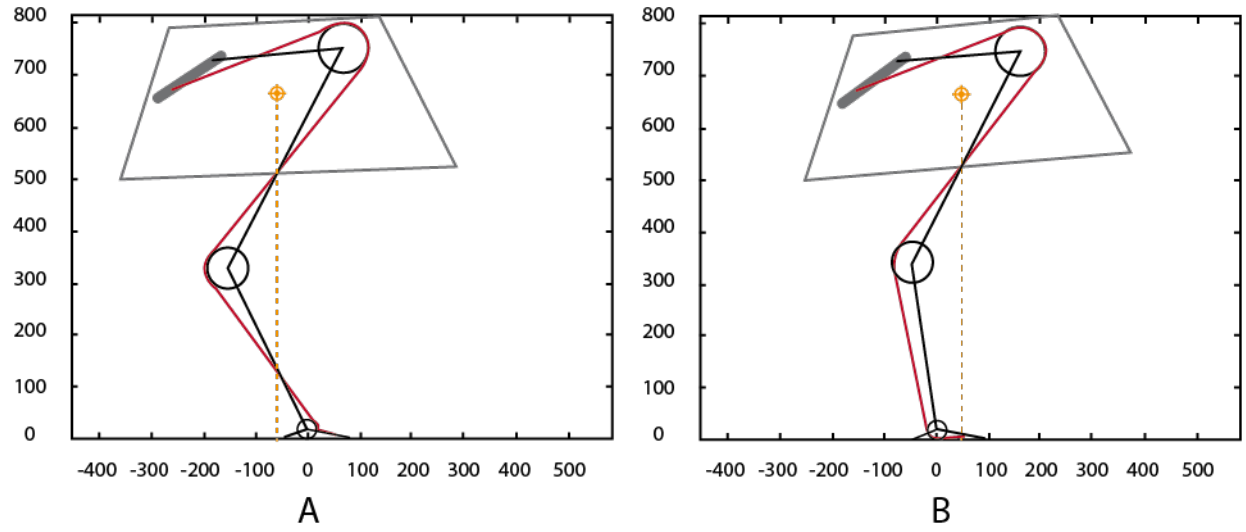

Figure 3 Two configurations of the system at equilibrium with the cable passing in front or behind the pulley of the toe joint.

Mathematical model with 4 cables

Anatomical data (Fig. 4)

Referring to the mean fibres of the muscles of the bird's leg (George & Berger 1966, Abourachid 1991), and considering the muscles involved in the extension of the leg corresponding to the previous cable, we observe that:

1) At the level of the knee and starting from the post-acetabular part of the pelvis, muscles operate the knee :

- 1- from the front by attaching to the patella. The patella is attached to the tibiotarsal crest by the patellar ligament.
- 2- from behind by the tendon of the iliofibular muscle, which passes through a ligamentous loop (*Ansa iliofibularis*) that connects the femur and the tibiotarsus at the back of the knee.

2) At the ankle, large heads of the muscle *gastrocnemius* join the tibiotarsus to the tarsometatarsus through the back of the ankle.

3) The toe flexors connect the tibiotarsus to the toes along the back of the ankle and the plantar aspect of the metatarsophalangeal joint. The anterior position the centre of rotation of the pulley is achieved by the anterior projection of the toe III trochlea.

Mathematical model (figure 4)

By considering these different muscle groups, we arrive at the model shown in Figure 4. B.

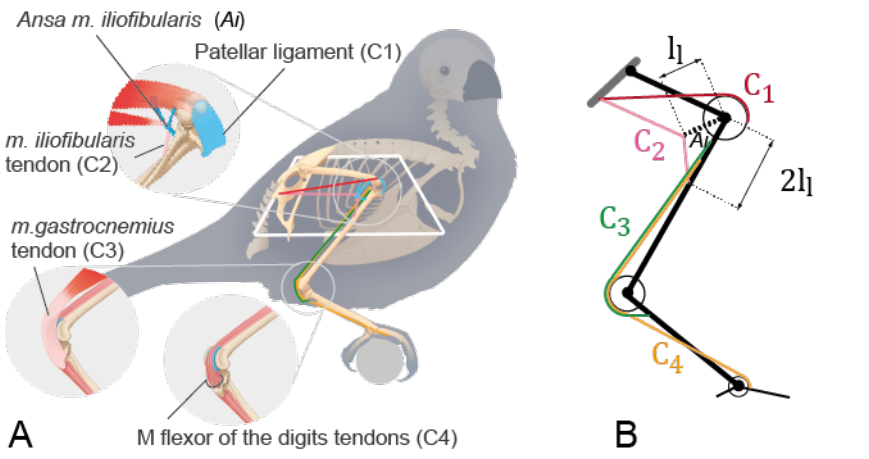

Figure 4 Model with four cables Anatomical features (A) used in the model with four cables (B) (Drawing by Camille Degardin)

Hip: Two cables (C1 and C2) are modelled attached to the pelvis at the same level as the single cable and have the same effect on the hip.

Knee: One cable (C1) passes through the front of the knee K by attaching to the patella, it is considered to be guided and attached by a pulley as in the previous model. Another cable (C2) passes K through a ligament loop (Ai) behind the knee. This ligament loop allows the cable to be held close to the joint and can be considered as a guided pulley. This loop is shown as a free segment of length l_l connecting the lower cable to the knee joint

At the ankle, a monoarticular cable (C3) passes the ankle only, and a biarticular cable (C4) passes the ankle and the foot joint. Cables 3 and 4 are assumed to be guided by the same pulley r_A as in the previous model.

The orientation of the segment representing the ligament loop is adjusted each time to minimise the length of the cable C2. This cable is attached to the tibiotarsus at a distance $2l_l$ from the knee joint. A refined simplified representation of our system is therefore presented in Figure 4. For simplicity (to limit the number of parameters in the model) it is assumed that the bi-articular finger-ankle tendon and the mono-articular ankle tendon are guided by the same pulley as in the previous model.

Using the same approach as before, we write the lengths of the 4 cables according to the configuration of the bird:

$$\begin{cases} l_{PA}(\boldsymbol{q}) = l_{0PA} + s_P r_P q_P - r_A q_A \\ l_A(\boldsymbol{q}) = l_{0A} - r_A q_A \\ l_{KH1}(\boldsymbol{q}) = l_{0KH1} + r_K q_K + l_H(q_H) \\ l_{KH2}(\boldsymbol{q}) = l_{KH2}(q_K, q_H) \end{cases}$$

Then, by writing the potential energy and considering the variations of the lengths of the cables as a function of the joint variables, we obtain

$$\begin{bmatrix} x_{CoM} - x_P \\ x_{CoM} - x_A \\ x_{CoM} - x_K \\ x_{CoM} - x_H \end{bmatrix} + \begin{bmatrix} s_P r_P \\ -r_A \\ 0 \\ 0 \end{bmatrix} \frac{F_{PA}}{mg} + \begin{bmatrix} 0 \\ -r_A \\ 0 \\ 0 \end{bmatrix} \frac{F_A}{mg} + \begin{bmatrix} 0 \\ 0 \\ r_K \\ -r_H(q_H) \end{bmatrix} \frac{F_{HK1}}{mg} + \begin{bmatrix} 0 \\ 0 \\ -r_{K2}(q_k, q_H) \\ -r_{H2}(q_k, q_H) \end{bmatrix} \frac{F_{HK2}}{mg} = \begin{bmatrix} 0 \\ 0 \\ 0 \\ 0 \end{bmatrix}$$

where F_{PA} is the tension in the toe-ankle cable, F_A is the tension in the ankle cable, F_{HK1} is the tension in the upper hip-knee cable and F_{HK2} is the tension in the lower hip-knee tendon. These forces are due to the elongation of the elastic cables under the effect of gravity, taking into account their chosen free length.

When a cable does not pass through a pulley, the lever arm is **defined by the minimum distance between the joint and the cable**. To make interpretation easier, we will record these lever arms as radii of pulleys of varying sizes. For the contribution of the cable C1 around the hip, we write : $\frac{\partial l_H(q_H)}{\partial q_H} = -r_H(q_H)$ with $r_H(q_H) > 0$ as for the previous

model. This means that the C1 cable is going to provide a negative torque around the hip. The hip and knee angles determine the length of the C2 cable.

We introduce the notations: : $\frac{\partial l_{KH2}(q_K,q_H)}{\partial q_H} = -r_{H2}(q_k,q_H)$, with $r_{H2}(q_k,q_H) > 0$ and $\frac{\partial l_{KH2}(q_K,q_H)}{\partial q_k} = -r_{K2}(q_k,q_H)$ avec $r_{K2}(q_k,q_H) > 0$. This means that the C2 cable will provide negative torque around the hip and knee.

If we write that each of the forces F_{PA} , F_A , F_{HK1} , F_{HK2} is proportional to a force F we obtain as equation :

$$\begin{bmatrix} x_{CoM}-x_P \\ x_{CoM}-x_A \\ x_{CoM}-x_K \\ x_{CoM}-x_H \end{bmatrix} + \begin{bmatrix} s_P r_P \frac{F_{PA}}{F} \\ -r_A \frac{F_{PA}}{F} - r_A \frac{F_A}{F} \\ r_K \frac{F_{HK1}}{F} - r_{K2}(q_k,q_H) \frac{F_{HK2}}{F} \\ -r_H(q_H) \frac{F_{HK1}}{F} - r_{H2}(q_k,q_H) \frac{F_{HK2}}{F} \end{bmatrix} \frac{F}{mg} = \begin{bmatrix} 0 \\ 0 \\ 0 \\ 0 \end{bmatrix}$$

We find the same equation as for the single-cable model (1), but with different geometric characteristics that represent the additions of the new model: the C2 cable that passes through the ligament loop and the C3 monoarticular cable of the ankle

In the single cable model only one force is applied. We maintain this assumption by applying the same force to all cables.

$$\begin{bmatrix} x_{CoM}-x_P \\ x_{CoM}-x_A \\ x_{CoM}-x_K \\ x_{CoM}-x_H \end{bmatrix} + \begin{bmatrix} s_P r_P \\ -2\boldsymbol{r_A} \\ \boldsymbol{r_K - r_{K2}(q_k,q_H)} \\ \boldsymbol{-r_H(q_H) - r_{H2}(q_k,q_H)} \end{bmatrix} \frac{F}{mg} = \begin{bmatrix} 0 \\ 0 \\ 0 \\ 0 \end{bmatrix} \quad (6)$$

Compared to the single-cable model:

1- It allows the position of the centre of mass to be constrained. As the radius of the ligament pulley of cable 2 is greater than the radius of the knee pulley, their sum is negative and moves the centre of mass forward to the knee in the balance position.

2- The radius of the ankle pulley counted for each cable is larger overall, allowing the ankle to move backwards away from the CoM. The position of point P does not change since there is only one cable as in the previous model.

If we choose $l_l = 1.8\, r_K$, with the measured anatomical parameters and the measured CoM position and $s_P = 1$, the configuration shown in Figure 5 is obtained. The ligament loop produces a guide for the tendon which is not the same as a pulley, since the radius of the equivalent pulley varies with the angle of the knee. Around the equilibrium positions we are studying, the

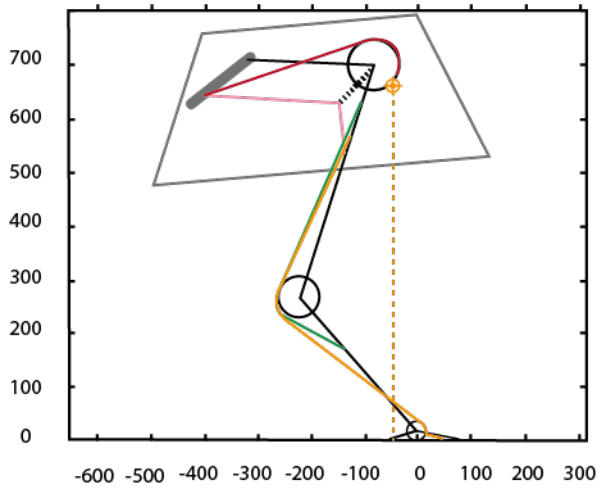

Figure 5: Equilibrium configuration resulting from equation (6) parameterised with the measurements in Table 1. The numerical simulation shows that the forces in the different cables are identical and correspond to approximately twice the weight of the bird. The stiffness matrix (equations (4), (5) and (7)) is used to check that this configuration is stable.

variation in cable length as a function of variations in angle q_K is smaller than for a pulley of size l_l. The value of l_l=1.8 r_K was chosen by testing and simulation to obtain a CoM position at the front of the knee that corresponds globally to observations. As this value increases, the CoM will be further forward of the knee at equilibrium. The stiffness and the free length of the cables have been chosen in such a way that the forces in the cables are the same.

The equilibrium configuration is closer to the *configuration measured on the zebrafinch model and shown in figure 2* than the configuration obtained with only 1 cable. It is also shown that a stable equilibrium can be obtained in this case. Other configurations can be calculated using the Matlab code provided in SM 4.

Postural stability

The postural stability conditions are the same as before with the same $\boldsymbol{K_g}$ matrix, but $\boldsymbol{K_c}$ is modified. For simplicity (to reduce the number of parameters), the stiffnesses of the cables C3 and C4, noted as K, are assumed to be identical, while the stiffness of the cables C1 and C2 is noted as k. The stiffness K of C3 and C4 must be sufficient to compensate for the destabilising effect of gravity on the ankle and toe joints. The resulting stiffness matrix is :

$$\boldsymbol{K_c} = \begin{bmatrix} Kr_P^2 & -Kr_Pr_A & 0 & 0 \\ -Kr_Pr_A & 2Kr_A^2 & 0 & 0 \\ 0 & 0 & k\left(r_K^2 + r_H(q_H)^2 + NL1\right) & k\left(r_K r_H(q_H) + r_{K2}\left(q_k, q_H\right) r_{H2}\left(q_k, q_H\right)\right) \\ 0 & 0 & k\left(r_K r_H(q_H) + r_{K2}\left(q_k, q_H\right) r_{H2}\left(q_k, q_H\right)\right) & k\left(r_H(q_H)^2 + r_{K2}\left(q_k, q_H\right)^2 + NL2\right) \end{bmatrix} \quad (7)$$

With $NL1 = \frac{\partial l_{HK2}^2(q_K, q_H)}{\partial^2 q_k}\left(l_{HK2}(q_K, q_H) - l_{v2}\right)$

and NL2= $\frac{\partial l_H^2(q_H)}{\partial^2 q_H}\left(l_{HK1}(q_K, q_H) - l_{v1}\right) + \frac{\partial l_{HK2}^2(q_K, q_H)}{\partial^2 q_H}\left(l_{HK2}(q_K, q_H) - l_{v2}\right)$

It can be seen that, compared to the single cable model, some off-diagonal terms have disappeared and that on the diagonal the 2^e row - 2^e column term is multiplied by 2. In this case it is possible to find a value of K that ensures stability.

In summary, the 4-cable system achieves a balance with the centre of gravity in front of, or near the knee with the C1 cable passing through the front of the knee pulley via the patellar ligament and C2 at the back through the *iliofibularis* loop. This dual system allows the size of the knee pulley to be reduced. Stability is adjusted thanks to the two cables C3 and C4 that pass the ankle. Passing C4 anterior or posterior to the centre of rotation of P adjusts the obliquity of the tarsometatarsus. The stiffness of cables C3 and C4 must be sufficient to compensate for the destabilising effect of gravity.

The mechanical stability of the equilibrium, i.e. the the non-tilting of the assembly around an edge of the ground contact zone is ensured by maintaining the CoM along the x axis in the support zone. This is ensured at equilibrium by choosing a much smaller pulley at the ground contact point r_P than the support surface (see the first line of

equation (6)). It will be useful to study the acceptable disturbances and the evolution of the CoM in the transient phase. This will be the subject of further studies.

Discussion

The result shows that a system of 5 rigid bodies, articulated like the pelvic skeleton of a bird, driven by a single cable passively tensioned by the action of gravity on the centre of mass, is able to extend the leg and reach equilibrium. The geometry of the knee joint (K), the ankle joint (A) and the metatarsophalangeal joint (P) therefore plays a crucial role in the system. If we think of them as pulleys, the radius of the pulleys determines the length of the joint lever arms and allows the cable to slide. The radius of the pulleys in the K and A joints is crucial for achieving equilibrium with minimum effort. Balance requires the centre of gravity of the body to be close to the vertical of the foot joint P, slightly in front of or slightly behind the centre of the pulley.

However, the single cable model, based on the proportions of the zebra finch at rest, only allows equilibrium when the CoM is placed behind the knee. However, the equilibrium is not stable and does not correspond to reality because the bird's CoM position is towards the centre of the trunk and in front of the knee.

A tensegrity system

One solution to achieve stability, i.e. the automatic return to equilibrium after a disturbance, is to have two extensor cables at the knee, one at the front of the pulley and one at the back, and two extensor cables at the ankle, one monoarticular and one pluriarticular. The latter also passes through the metatarsophalangeal joint to attach to the foot. The two cables that pass through the hip and knee allow the centre of mass to be moved forward. The ankle system provides stability to the system. The cable routing at the foot allows the degree of flexion of this joint to be adjusted. The four-cable solution is sufficient to have a stable posture if the radii of the pulleys are adjusted. There are other solutions that we have not described in detail. For example, a monoarticular cable at the front of the ankle and of the monoarticular cable at the knee will also provide stable posture. The mathematical explanation of this possibility is provided as supplementary material [SM2].

In this way, we have shown that the proposed four-cable model is equivalent to a tensegrity system. It is the tension of the cables (muscles-tendons) applied to rigid elements (bones) that provides the posture and static equilibrium of the osteomuscular system. The force of gravity applied to the centre of mass of the body passively puts the system under tension and ensures its stability.

Bipedal system unique to birds

Analysis of the evolution of the osteomuscular system on the line to crown-group birds (Hutchinson 2002) shows that features associated with our model appeared in the line from dinosaurs to birds. During birds evolution, the dorsal vertebrae have fused into a long synsacrum to which the ilium attaches cranially and the ischium and pubis caudally. The three pelvic bones are fused together at the acetabulum, the hip socket. The caudal extension of the pelvis allows the post acetabular muscles to attach far behind the hip, increasing the moment arm of these hip extensor muscles. The position of the centre of mass very anterior to the hip, induces the clockwise tension around the hip whether bird is standing. These two features, which are characteristic of birds, allow the pelvic system to be tensed under the action of gravity. The knee pulley, formed by the distal trochlea of the femur in which the patella slides, also exists in mammals, it has appeared twice. It appeared late in the avian lineage (Hutchinson 2002). The tibial ridge shape to which the patellar ligament attaches are also typical. They are large and increase the forward moment arm. The caudal position of the short cruciate ligaments and menisci show that the centre of rotation is shifted backwards in the knee joint, further increasing the lever arm and favouring the flexed position. The tendon loop that holds the tendon of the *iliofibularis* muscle plays a fundamental role for balance in our system as it combines with the patellar system to maintain posture with the centre of mass far anterior.

The ankle is in fact an intertarsal joint that appears in the avian lineage (Baumel 1993). It is formed by the tarsi, one part of which is fused to the tibia and the other part fused to the metatarsi, which are themselves fused together. The condyles of the tibiotarsus are projected cranially and rotate on the cotyls situated cranially on the hypotarsal plateau. On the distal caudal side of the tibiotarsus, a trochlea accommodates the tibial cartilage encased in the gastrocnemius tendon which inserts onto the hypotarsus. The tendons of the finger flexors slide under this tendon and into the tibial cartilage. The plantar side of the hypotarsus of the tarsometatarsus has a highly variable shape, from two ridges on either side of a groove to a complex system of more or less posteriorly projected ridges and channels (Mayr 2016). This diversity could correspond to the adjustments that allow postural diversity. The intertarsal joint is more or less flexed in birds at rest. It is tense in waders, for example, and flexed in passerines such as the zebra finch. The intertarsal joint also shows peculiarities on its anterior surface, with a system of retinaculum and bony bridges that allow the sliding of tendons. These tendons could also contribute to the stability of the system.

Distally, the trochleae of the three metatarsals are not fused. Their orientation corresponds to the orientation of the toes (Abourachid et al, 2017; Leblanc 2023). The trochlea of metatarsal III may or may not be offset forwards. This morphological diversity must also participate in postural adjustments, by modifying the trajectory of the tendons in relation to the centre of rotation of the joint.

Stiffness of the cables

The wiring corresponds to the muscle system in the hind limbs. This is a very complex system with over 40 muscles. Many of these are multi-jointed and many have multiple heads (George & Berger 1966). This system allows adaptation to all situations encountered in the animal's life, far beyond the maintenance of posture. Locomotor constraints particularly affect the leg muscles. They are used in a variety of conditions in birds, both in movement, walking, running, swimming, take-off and landing, and in relation to substrates, water, soil and vegetation. The mechanical constraints are therefore very different depending on the ecology of the species. Our modelling ignores this complexity to keep only the elements necessary for postural stability. As the bipedal position is the resting posture of birds, stiffness should be ensured with a minimum of control and fatigue. There is a relay of aponeutic in the thigh musculature, which join distally to participate in the patellar tendon. There are also aponeutic-tendinous relays in the flexor and gastrocnemius muscles. Together with the tendons, muscle fascia and extracellular matrix (Csapo & al 2020), these collagen-rich tissues could be involved in the stiffness of the cables, as collagen gives the tissues mechanical stability, strength and toughness (Fratzl 2008). Articular cartilage is also rich in collagen fibres (Bielajew et al 2021). The tibial cartilage, which is unique to birds , may therefore have a role in the tension of the intertarsal joint. In birds, some deep tendons in the leg and tarsus are calcified (Baumell 1993). Tendon calcification only occurs in the straight parts of the tendon, the parts that slide in the joints remain flexible. This tendency to calcify tendons is also unique to birds. It increases the Young's modulus and stiffness of calcified tendons, which is of interest in the case of economic tension (Bennet and Stafford 1998). These calcifications are found in our C3 and C4 cables, which need to be stiff to ensure stable posture

Tensegrity and evolution

Within evolutionary biology, some morphological characters are more important than others. These are evolutionary innovations, new characters that have been selected for by evolution and that are conserved and shared by the descendants of the same lineage (synapomorphy - Henig 1965). Synapomorphies are well identified in birds (Clarke and Middleton 2008). Some characteristics identified as necessary for postural stability in our study are synapomorphies. The plan of organisation of the body that allows balance to be achieved with a single-cable system is one (Gatesy & Middleton 1998, Abourachid & Hofling 2012). The iliofibular tendinous loop, tibial ridges or hypotarsal canals required for postural stability in the 4-cable system are synapomorphies (Hutchinson 2002). We propose that tensegrity, which allows light and stable mechanical systems, is fundamental to the evolution of the avian body plan. Within this framework, joint shape and size would be critical for understanding functional

adaptations in evolutionary biology The concept of tensegrity opens up a new paradigm for the functional interpretation of morphological features. It may also have applications in the modelling of the equilibrium of extinct species.

Tensegrity and artificial selection

Identifying the function of traits selected by natural evolution is also important in the context of artificial selection. Selection of individuals with morphological traits of commercial interest, such as pectoral muscle size in poultry, alters the overall balance of the system (Abourachid 1991, 1993, Stover 2018), leading to lameness and animal suffering. Awareness of the imbalances caused by artificial selection should improve the living conditions of domestic species.

Interest of this study for robotics

The vast majority of bipedal robot platforms are inspired by human models, and at rest bipedal robots are straight legged. However, these balance configurations are not stable and the standard model for walking (Kajita et al., 2014) is an inherently unstable inverted pendulum model (the feet are reduced to points). This implies that the walking pattern consists of a sequence of instabilities that must be judiciously assembled to generate stable gaits (Chevallereau et al. 2003). The introduction of mechanically stable resting structures could provide a new perspective on the study of bipedal walking. Even the most bio-inspired structures currently available do not have these stable passive equilibrium configuration properties (Badri-Spröwitz et al. 2022). Another application directly inspired by birds is to equip legged drones to maintain a fixed posture for periods of observation or inspection without using energy (Doyle et al. 2011). Avian bipedalism in tension is very different from human bipedalism in compression. This result can also be used as an alternative for the design of human-like bipedal robots.

Conclusion

This work opens a new paradigm for the morpho-functional study of the evolution of the avian lineage by proposing tensegrity as a new biomechanical framework. The basis of postural stability in birds can be considered as tensegrity. The rigid bones can be held together by tensions in tendons and collagen tissues. Pelvic shape and joint geometry play a fundamental role in postural balance, while tendon pathways allow for economic stability. The parameters of this system could be adjusted, such as the size of the pulleys, the length of the cables or their stiffness, without losing the inherent postural stability. This system could have allowed the geometry of the osteomuscular system to be adjusted over the course of evolution to adapt to the diversity of living environments and behaviours of the 10,000 species of birds.

This initial work does not answer all the questions and will need to be pursued. This initial work relies on a single bird species. Bird morphological diversity needs to be measured, different parameter sets explored and limits tested.. This analysis is static and needs to be extended by studying the transient and dynamic behaviour of the system. An extension to a spatial model is also important.

Acknowledgment:

This project has received financial support from the CNRS through the MITI interdisciplinary programs.

References

Abourachid, A. (1991). Comparative gait analysis of two strains of turkey, *Meleagris gallopavo*. British Poultry Science, 32(2), 271-277.

Abourachid, A. (1993). Mechanics of standing in birds: functional explanation of lameness problems in giant turkeys. British poultry science, 34(5), 887-898.

Abourachid, A., & Höfling, E. (2012). The legs: a key to bird evolutionary success. Journal of Ornithology, 153, 193-198.

Abourachid, A., Hugel, V. (2015) L'idée de fonction en biologie et en robotique, témoignage autour du projet " RoboCoq ". in Les fonctions : des organismes aux artefacts.Gayon J, De Ricqles,A edt Presses universitaires de France

Abourachid, A., Fabre, A. C., Cornette, R., & Höfling, E. (2017). Foot shape in arboreal birds: two morphological patterns for the same pincer-like tool. Journal of anatomy, 231(1), 1-11.

Alexander, R. M., & Dimery, N. J. (1985). The significance of sesamoids and retro-articular processes for the mechanics of joints. Journal of Zoology, 205(3), 357-371.

Allen, V., Bates, K. T., Li, Z., & Hutchinson, J. R. (2013). Linking the evolution of body shape and locomotor biomechanics in bird-line archosaurs. *Nature*, *497*(7447), 104-107. https://doi.org/10.1038/nature12059

Baumel, J. J. (1993). Handbook of avian anatomy: nomina anatomica avium. Harvard University Press Publications of the Nuttall Ornithological Club Massachusetts (USA). no. 23

Badri-Spröwitz, A., Sarvestani, A.A., Metin S. M. and Daley, M.A. (2022) BirdBot achieves energy-efficient gait with minimal control using avian-inspired leg clutching, Science Robotics, vol. 7, No. 64

Bennett, MB, Stafford J A. 1988. Tensile properties of calcified and uncalcified avian tendons. *Journal of Zoology*, *214*(2), 343-351.

Bielajew, B. J., Hu, J. C., & Athanasiou, K. A. (2020). Collagen: quantification, biomechanics and role of minor subtypes in cartilage. Nature Reviews Materials, 5(10), 730-747.

Boas, J.E.V., 1933. Kreuzbein, Becken und Plexus lumbosacralis der Vögel. Mémoires de l'Académie Royale des Sciences et des Lettres de Danemark, Section des Sciences 5, 1-74.

Carter, D. R., Fyhrie, D. P., & Whalen, R. T. (1987). Trabecular bone density and loading history: regulation of connective tissue biology by mechanical energy. Journal of biomechanics, 20(8), 785-794.

Csapo, R., Gumpenberger, M., & Wessner, B. (2020). Skeletal muscle extracellular matrix–what do we know about its composition, regulation, and physiological roles? A narrative review. Frontiers in physiology, 11, 253.

Chang, Y. H., & Ting, L. H. (2017). Mechanical evidence that flamingos can support their body on one leg with little active muscular force. Biology Letters, 13(5), 20160948.

Chevallereau, C, Abba, G., Aoustin, Y., Plestan, F., Westervelt, E.R., Canudas de Wit, C., Grizzle, J. W., (2003), Rabbit: A Testbed for Advanced Control Theory, IEEE Control Systems Magazine, vol. 23, no. 5, pp 57-79.

Cignoni, P., Ranzuglia, G., Callieri, M., Corsini, M., Ganovelli, F., & Pietroni, N. (2011). MeshLab.

Clarke, J. A., & Middleton, K. M. (2008). Mosaicism, modules, and the evolution of birds: results from a Bayesian approach to the study of morphological evolution using discrete character data. Systematic biology, 57(2), 185-201.

do Rosário, J. L. P. (2014). Biomechanical assessment of human posture: a literature review. *Journal of bodywork and movement therapies*, *18*(3), 368-373.

Doyle, C. E., Bird, J. J., Isom, T. A., Johnson, C. J., Kallman, J. C., Simpson, J. A. & Minor, M. A. (2011, September). Avian-inspired passive perching mechanism for robotic rotorcraft. In *Intelligent Robots and Systems (IROS), 2011 IEEE/RSJ International Conference on* (pp. 4975-4980).

Fratzl, P. (2008). Collagen: structure and mechanics, an introduction. In Collagen: structure and mechanics (pp. 1-13). Boston, MA: Springer US.

Gatesy, S. M., & Middleton, K. M. (1997). Bipedalism, flight, and the evolution of theropod locomotor diversity. Journal of Vertebrate Paleontology, 17(2), 308-329.

Galton, P. M., & Shepherd, J. D. (2012). Experimental analysis of perching in the European starling (Sturnus vulgaris: Passeriformes; Passeres), and the automatic perching mechanism of birds. Journal of Experimental Zoology Part A: Ecological Genetics and Physiology, 317(4), 205-215.

George JC, Berger AJ. 1966 Avian myology New York and London Academic Press 500pp

Harvey, C., Baliga, V. B., Wong, J. C. M., Altshuler, D. L., & Inman, D. J. (2022). Birds can transition between stable and unstable states via wing morphing. *Nature*, *603*(7902), 648-653.

Hennig, W. (1965). Phylogenetic systematics. Annual review of entomology, 10(1), 97-116.

Höfling, E., & Abourachid, A. (2021). The skin of birds' feet: Morphological adaptations of the plantar surface. *Journal of Morphology*, *282*(1), 88-97. **https://doi.org/10.1002/jmor.21284**

Hutchinson, J. R. (2002). The evolution of hindlimb tendons and muscles on the line to crown-group birds. Comparative Biochemistry and Physiology Part A: Molecular & Integrative Physiology, 133(4), 1051-1086

Ingber, D. E., Wang, N., & Stamenović, D. (2014). Tensegrity, cellular biophysics, and the mechanics of living systems. Reports on Progress in Physics, 77(4), 046603.

Kajita, S., Hirukawa, H., Harada, K.Yokoi, K., (2014) Introduction to Humanoid Robotics, Springer Tracts in Advanced Robotics, Springer Berlin Heidelberg.

Leblanc, K., Pintore, R., Galvão, A., Heitz, E., & Provini, P. (2023). Foot adaptation to climbing in ovenbirds and woodcreepers (Furnariida). *Journal of Anatomy*, *242*(4), 607-626.

Mayr, G. (2016). Variations in the hypotarsus morphology of birds and their evolutionary significance. *Acta Zoologica*, *97*(2), 196-210.

Provini, P., & Abourachid, A. (2018). Whole-body 3D kinematics of bird take-off: key role of the legs to propel the trunk. The Science of Nature, 105(1-2), 12.

Raikow, R. J. (1985). Locomotor system. *Form and function in birds*, *3*, 57-147.

Snelson the reference is complete. It is the patent US 3169611 as entionned. It can be found here. https://patentimages.storage.googleapis.com/3c/0f/03/39e41d62efddd8/US3169611.pdf

Stover, K. K., Brainerd, E. L., & Roberts, T. J. (2018). Waddle and shuffle: gait alterations associated with domestication in turkeys. Journal of Experimental Biology, 221(15), jeb180687.

Swanson, R. L. (2013). Biotensegrity: a unifying theory of biological architecture with applications to osteopathic practice, education, and research-a review and analysis. Journal of Osteopathic Medicine, 113(1), 34-52.

Tardieu, C., Bonneau, N., Hecquet, J., Boulay, C., Marty, C., Legaye, J., & Duval-Beaupère, G. (2013). How is sagittal balance acquired during bipedal gait acquisition? Comparison of neonatal and adult pelves in three dimensions. Evolutionary implications. *Journal of human evolution*, *65*(2), 209-222.

Wenger, P, Chablat, D. (2019). Kinetostatic analysis and solution classification of a class of planar tensegrity mechanisms. Robotica, *37*, 1214-1224.

Wenger, P., Fasquelle, B., Abourachid, A., & Chevallereau, C. (2023). A tensegrity robot inspired from the bird neck. Techniques de l'ingénieur-Bio-inspired robotics. S 7 858 -